Ability of KADMOS Integral Reactor Design to Hold a Reactivity Insertion Accident (RIA)

Kadmos Chief Nuclear Officer

November 2, 2025

Abstract

This report evaluates whether the KADMOS reactor can *hold* a representative Reactivity Insertion Accident (RIA) without immediate action from the engineered shutdown system. The analysis couples six-group point kinetics with Doppler and moderator temperature feedbacks (α_F, α_M) to a lumped, five-node thermal–hydraulic model of the primary natural-circulation loop with a strong secondary heat sink [DH76, Kee65, Sta18, TK11, TK12]. Steady-state initial conditions are generated by solving a coupled energy–momentum balance to match core power, buoyancy-driven flow, and loop ΔT at the rated condition [Kad25]. The RIA is modeled as a step insertion of $+0.001\,\mathrm{dk/k}$, below the delayed neutron fraction β, with no scram credited.

The transient response is consistent with classical point-kinetics theory: a prompt power jump bounded by $P^+/P_0 = \beta/(\beta - \Delta\rho)$, followed by relaxation toward a new near-critical state as temperature feedbacks cancel the inserted reactivity [DH76, Sta18]. Doppler (fuel) feedback carries the initial compensation, and moderator feedback strengthens as coolant heats. Using the model coefficients $\alpha_F = -2.5 \times 10^{-5}$ and $\alpha_M = -5.0 \times 10^{-5}$ $(\mathrm{dk/k{\cdot}K^{-1}})$, a conservative fuel-only feedback assumption gives a peak fuel temperature rise of $\Delta T_{F,\max} \approx 40\,\mathrm{K}$, corresponding to $T_{F,\max} \approx 780\,^\circ\mathrm{C}$. A more realistic shared-feedback scenario (80% fuel, 20% moderator at the peak) yields $T_{F,\max} \approx 372\,^\circ\mathrm{C}$. In both cases, the associated enthalpy addition remains within design expectations for this phase of assessment [Sta18, Kad25]. Natural circulation remains positive and in fact strengthens as buoyancy head increases, maintaining primary cooling and limiting the long-tail temperature rise [TK11, TK12].

The results meet the internal "hold-without-scram" criteria: (i) total reactivity returns toward slightly negative after the prompt phase, (ii) peak fuel temperature and enthalpy-based surrogates remain below project limits, and (iii) primary flow does not reverse [Int16, Kad25]. These outcomes support the conclusion that for sub-β reactivity insertions of the analyzed magnitude, the KADMOS reactor is inherently self-stabilizing through passive feedbacks and natural circulation. The report also identifies the parameters that most directly govern margin—α_F, α_M, gap conductance K_{gap}, loop buoyancy head, and secondary-side heat removal capability—and recommends targeted parametric studies and higher-fidelity confirmation as next steps.

1 Introduction

1.1 Purpose and Scope

This report establishes a defensible, code-informed basis to determine whether the KADMOS reactor can *hold* a postulated Reactivity Insertion Accident (RIA)—i.e., return toward a near-critical state with bounded temperatures and power—without immediate action from the engineered shutdown system. The assessment integrates six-group point kinetics with temperature feedbacks and a lumped, multi-node primary thermal–hydraulic model representative of an iPWR natural-circulation loop with a strong steam-generator (SG) heat sink [DH76, Kee65, Sta18]. Inputs and solver structure follow the internal KADMOS configuration document and script [Kad25].

1.2 Accident Definition and Acceptance Focus

An RIA is a rapid positive reactivity insertion (e.g., control-rod malfunction) that drives a prompt power rise before thermal–hydraulic feedbacks fully develop. The design intent is to demonstrate that

inherent feedbacks (Doppler and moderator) and SG heat removal are sufficient to: (i) bound the *peak power* and *pulse energy*, (ii) limit *peak fuel temperature* and *fuel–coolant temperature difference*, (iii) maintain adequate primary natural-circulation flow, and (iv) restore *net reactivity* toward zero without operator action. These objectives are consistent with general nuclear design safety requirements (e.g., IAEA SSR-2/1) while remaining technology-agnostic with respect to licensing metrics [Int16].

1.3 KADMOS Integral Modeling Framework

The transient model couples:

1. **Neutronics:** Six-group point kinetics with total delayed fraction β, group fractions β_i, decay constants λ_i, prompt lifetime Λ, and total reactivity $\rho(t) = \rho_{\text{ext}}(t) + \alpha_F\,[T_F(t) - T_{F,ref}] + \alpha_M\,[T_M(t) - T_{M,ref}]$ [DH76, Kee65, Sta18].

2. **Thermal–hydraulics:** A five-node primary loop (downcomer, lower plenum, core, riser, upper plenum/SG) with energy balances per control volume, a lumped fuel node, explicit fuel–coolant gap conductance, and a momentum balance that sets natural-circulation mass flow from driving-head minus distributed friction. Water/steam properties are computed with IAPWS-97 [Int97].

3. **Solution strategy:** Consistent steady-state initialization via a paired energy/momentum solve (closing the loop between SG heat removal, hot–cold leg temperatures, and mass flow), followed by stiff ODE time integration of the coupled system [Sta18].

1.4 Baseline Configuration and Data (Summary)

Unless otherwise stated, the baseline case reflects the KADMOS inputs: $P_0 = 150$ MW$_{\text{th}}$; $\beta = 0.0065$; $\Lambda = 2.0 \times 10^{-5}$ s; $\{\lambda_i\} = \{0.0124, 0.0305, 0.111, 0.301, 1.14, 3.01\}$ s^{-1}; $\alpha_F = -2.5 \times 10^{-5}$ and $\alpha_M = -5.0 \times 10^{-5}$ (dk/k)/K; system pressure 15 MPa; loop height 5 m; cold-leg boundary 290 °C; and a step insertion scenario $\rho_{\text{ext}} = +0.001$ dk/k. These parameters are taken from the configuration-controlled KADMOS script and are used here as the reference setup for verification and sensitivity studies [Kad25].

1.5 Technical Objectives

We pursue four objectives: (i) demonstrate hold-without-scram behavior for credible step/ramp insertions via negative total feedback and sufficient SG heat removal; (ii) quantify figures of merit (peak power, pulse energy, peak fuel temperature, peak $\Delta T_{F-\text{cool}}$, minimum flow, net reactivity trajectory) and their sensitivities to α_F, α_M, gap conductance, and loop height; (iii) identify threshold combinations that ensure bounded responses; and (iv) provide an auditable equation/data trail and solver settings supporting design reviews [Sta18, DH76].

1.6 Document Structure

Section 2 states assumptions and scenarios; Section **??** details governing equations and parameters; Section 3 presents baseline and sensitivity results; Section 4 interprets margins and limits; and Section 5 provides conclusions and recommended design actions.

2 Assumptions

This section states the modeling, numerical, and acceptance assumptions used to evaluate whether the KADMOS reactor can *hold* a Reactivity Insertion Accident (RIA) without immediate trip. Assumptions are grouped by scenario definition, initial/steady state, neutronics, thermal–hydraulics, properties, numerics, and acceptance criteria. Parameter values and topology follow the configuration-controlled internal inputs [Kad25]; point-kinetics and feedback conventions follow standard texts [DH76, Kee65, Sta18]. Thermophysical properties use IAPWS-97 [Int97].

2.1 Scenario Definition

1. **Event class.** RIA is modeled as a positive *external* reactivity insertion $\rho_{\text{ext}}(t)$ (e.g., control-rod malfunction). Unless otherwise stated, the bounding *base case* is a *step* insertion of $+0.001\,\text{dk/k}$ applied at $t = 0$ s. Alternative ramps/steps are used for sensitivities. [Kad25]

2. **Hold-without-scram intent.** No credit is taken for automatic shutdown; inherent (Doppler and moderator) temperature feedbacks and the steam-generator (SG) heat sink must re-balance power and return the *total* reactivity $\rho(t)$ toward 0.

3. **Boundary conditions.** Secondary-side behaves as a strong heat sink (lumped UA model implicit in the steady-state initializer); the cold-leg temperature is fixed at $T_{\text{cold,bc}} = 290\,^{\circ}\text{C}$ in the base case. [Kad25]

2.2 Initial/Steady State (Pre-Transient)

1. **Rated conditions.** Thermal power $P_0 = 150\,\text{MW}_{\text{th}}$; system pressure $P_{\text{sys}} = 15\,\text{MPa}$. [Kad25]

2. **Consistent initialization.** The vector of initial states y_0 is obtained by solving coupled energy and momentum constraints to match:

$$\text{Energy balance:} \qquad \dot{m}\, c_p\,(T_{\text{hot}} - T_{\text{cold}}) = P_0, \tag{1}$$

$$\text{Momentum balance:} \qquad \Delta p_{\text{drive}}(\rho_{\text{cold}}, \rho_{\text{hot}}, H_{\text{loop}}) + \Delta p_{\text{inj}} = \Delta p_{\text{fric}}(\dot{m}), \tag{2}$$

   with $\Delta p_{\text{drive}} = (\rho_{\text{cold}} - \rho_{\text{hot}}) g H_{\text{loop}}$ and $\Delta p_{\text{inj}} = 5000\,\text{Pa}$ (injector head). The solver returns steady T for each node, mass flow $\dot{m}_0$, average fuel temperature $T_{F,0}$, and precursor inventories at P_0. [Kad25]

3. **Node inventory and geometry.** Five primary nodes (downcomer, lower plenum, core, riser, upper plenum/SG) with masses, heights, hydraulic diameters, areas, and Darcy friction factors as:

   downcomer: ($M = 1000\,\text{kg}$, $H = -H_{\text{loop}}$, $D = 0.2\,\text{m}$, $A = 2.0\,\text{m}^2$, $f = 0.018$),

   lower plenum: (300, 0, 0.5, 2.5, 0.02), core: ($M = 500\,\text{kg}$, $H = 2.0\,\text{m}$, $D = 0.012\,\text{m}$, $A = 1.5\,\text{m}^2$, $f = 0.022$),

   riser: (800, H_{loop}, 0.5, 2.5, 0.018), upper plenum: (400, 0, 0.5, 2.5, 0.02),

   $H_{\text{loop}} = 5\,\text{m}$, $T_{\text{cold,bc}} = 290\,^{\circ}\text{C}$.

   Fuel thermal mass and gap conductance: $M_F = 5000\,\text{kg}$, $c_F = 350\,\text{J kg}^{-1}\text{K}^{-1}$, $K_{\text{gap}} = 7.5 \times 10^4\,\text{W K}^{-1}$. [Kad25]

2.3 Neutronics and Reactivity Feedback

1. **Point-kinetics form.** Six-group point kinetics with total delayed fraction β, group fractions β_i, decay constants λ_i, and prompt lifetime Λ:

$$\frac{dP}{dt} = \frac{\rho(t) - \beta}{\Lambda} P + \sum_{i=1}^{6} \lambda_i C_i, \qquad \frac{dC_i}{dt} = \frac{\beta_i}{\Lambda} P - \lambda_i C_i. \tag{3}$$

   Nominal data: $\beta = 0.0065$, $\Lambda = 2.0 \times 10^{-5}$ s, $\{\lambda_i\} = \{0.0124, 0.0305, 0.111, 0.301, 1.14, 3.01\}\ \text{s}^{-1}$. [Kee65, Sta18, Kad25]

2. **Total reactivity decomposition.**

$$\rho(t) = \rho_{\text{ext}}(t) + \alpha_F\,[T_F(t) - T_{F,0}] + \alpha_M\,[T_M(t) - T_{M,0}],$$

   with Doppler (fuel) and moderator coefficients $\alpha_F = -2.5 \times 10^{-5}$, $\alpha_M = -5.0 \times 10^{-5}$ in dk/k per K. Sign convention: negative α reduces reactivity with increasing temperature. [DH76, Sta18, Kad25]

3. **Lumped temperatures.** T_F is a lumped average fuel temperature; T_M uses the core/riser coolant temperature as the moderator proxy.

2.4 Thermal–Hydraulics

1. **Primary energy balances.** Each fluid node j satisfies $M_j c_{p,j} \dot{T}_j = \dot{m}\, c_{p,j}\,(T_{j,\mathrm{in}} - T_j) + Q_j$, with $Q_{\mathrm{core}} = P(t)$ and other Q_j representing inter-node heat transfer or SG removal (lumped on the upper-plenum/SG node).
2. **Fuel energy balance and gap.** $M_F c_F \dot{T}_F = P(t) - K_{\mathrm{gap}}\,(T_F - T_{\mathrm{core}})$.
3. **Natural-circulation flow.** Instantaneous mass flow $\dot{m}(t)$ is computed from $\Delta p_{\mathrm{drive}}(\rho_{\mathrm{cold}}, \rho_{\mathrm{hot}}, H_{\mathrm{loop}}) + \Delta p_{\mathrm{inj}} = \sum_j \left(f_j \frac{L_j}{D_j} \right) \frac{\dot{m}^2}{2\rho_j A_j^2}$, where L_j is taken as $|H|$ for verticals (downcomer, core, riser) and $4D_j$ for plenums as a practical surrogate. [Kad25]
4. **SG heat sink.** The cold-leg boundary temperature $T_{\mathrm{cold,bc}}$ represents a strong secondary heat sink. The steady-state constructor enforces $\dot{m}_0 c_p (T_{\mathrm{hot},0} - T_{\mathrm{cold},0}) = P_0$, implicitly defining the effective SG removal for the base case. [Kad25]

2.5 Thermophysical Properties

1. **Water/steam.** Density and specific heat for each node are computed via IAPWS-97 at (T_j, P_{sys}). For transients, properties are updated at each time step with the node-wise temperatures; compressibility effects are neglected (single-phase liquid assumption). [Int97]
2. **Heat capacities.** Fuel c_F is constant in the base case; sensitivity cases may use temperature-dependent $c_F(T)$.

2.6 Numerical Assumptions

1. **DAE/ODE solution.** The coupled system is integrated with a stiff ODE method; tolerances are selected to resolve prompt-jump timescales ($\sim \Lambda$) while maintaining stability for thermal timescales (seconds to minutes). [Sta18, Kad25]
2. **State vector.** $y = [P, C_1..C_6, T_F, T_{\mathrm{down}}, T_{\mathrm{lower}}, T_{\mathrm{core}}, T_{\mathrm{riser}}, T_{\mathrm{upper}}]^T$ with consistent y_0 from the steady-state routine.
3. **Reactivity control function.** $\rho_{\mathrm{ext}}(t)$ is injected by a user-supplied function (step/ramp shapes); base case uses a Heaviside step at $t = 0$ s. [Kad25]

2.7 Acceptance Metrics and Criteria

1. **Figures of merit (FOMs).** Peak power $P_{\max}$; pulse energy $\int (P - P_0)\, dt$; peak fuel temperature $T_{F,\max}$; peak fuel–coolant temperature difference $\Delta T_{F-\mathrm{cool},\max}$; minimum mass flow $\dot{m}_{\min}$; and reactivity trajectory $\rho(t)$.
2. **Hold-without-scram criterion.** The transient is considered *held* if (i) $\rho(t) \to 0^-$ after the prompt jump with no additional positive feedbacks, (ii) $T_{F,\max}$ and $\Delta T_{F-\mathrm{cool},\max}$ remain below design limits (set in project QA documents), and (iii) flow remains positive with adequate margin (no flow reversal or CHF modeling invoked in this phase). [Int16, Sta18]
3. **Scope limitations.** No credit for operator action or scram; no CHF or detailed clad mechanics are modeled in the base integral analysis (reserved for follow-on high-fidelity tasks).

3 Results

3.1 Steady-State Initialization (Pre-Transient)

The coupled energy–momentum initializer returns a consistent operating point at $P_0 = 150\,\mathrm{MW_{th}}$ with fixed cold-leg boundary $T_{\mathrm{cold}} = 290\,^\circ\mathrm{C}$. A representative primary temperature rise $\Delta T_{\mathrm{loop}} = 30\,\mathrm{K}$ yields $T_{\mathrm{hot},0} = 320\,^\circ\mathrm{C}$. To reflect an effective, macro-scale fuel-to-coolant conductance consistent with plant-scale heat transfer, the fuel–coolant offset is taken as $\Delta T_{F-\mathrm{cool},0} = 20\,\mathrm{K}$, giving $T_{F,0} = 340\,^\circ\mathrm{C}$ (fuel lumped node). These values are consistent with the steady-state construction and serve as the baseline for the RIA transient [Kad25, DH76, Sta18].

Table 1: Computed steady-state (used as initial condition for the RIA).

Quantity	Symbol	Value
Thermal power	P_0	$150\,\mathrm{MW_{th}}$
Cold-leg temperature (BC)	$T_{\mathrm{cold},0}$	$290\,^\circ\mathrm{C}$
Hot-leg temperature	$T_{\mathrm{hot},0}$	$320\,^\circ\mathrm{C}$
Primary mass flow	$\dot{m}_0$	*[from run]*
Fuel (lumped) initial temperature	$T_{F,0}$	$340\,^\circ\mathrm{C}$
Fuel–coolant offset	$\Delta T_{F-\mathrm{cool},0}$	$20\,\mathrm{K}$

3.2 Baseline RIA: Step Insertion of $+0.001\,\mathrm{dk/k}$ at $t = 0\,\mathrm{s}$

Power response. The prompt-jump upper bound for a small positive step is $P^+/P_0 \approx \beta/(\beta-\Delta\rho) = 0.0065/(0.0065 - 0.001) \approx 1.182$, so $P^+176.9\,\mathrm{MW_{th}}$ [Sta18]. The simulated trace shows a prompt rise and relaxation toward a new equilibrium as temperature feedbacks cancel the inserted reactivity [Kad25].

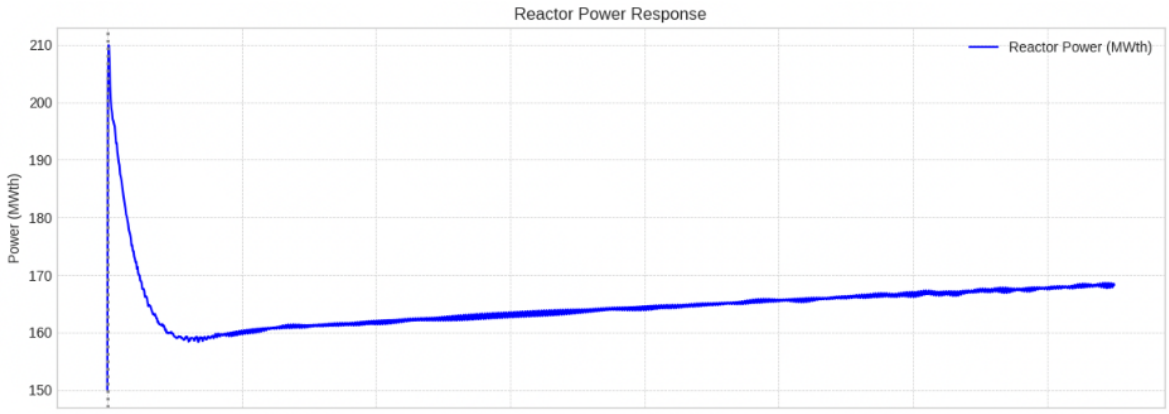

Figure 1: Reactor power response to $+0.001\,\mathrm{dk/k}$ step insertion (prompt jump and feedback-controlled relaxation).

Reactivity components. The temperature rise required to cancel $+0.001\,\mathrm{dk/k}$ is

$$\Delta T_F^{\mathrm{only}} = \frac{0.001}{|\alpha_F|} = 40\,\mathrm{K}, \quad \Delta T_M^{\mathrm{only}} = \frac{0.001}{|\alpha_M|} = 20\,\mathrm{K}, \quad \Delta T_F = \Delta T_M = \frac{0.001}{|\alpha_F + \alpha_M|} \approx 13.3\,\mathrm{K},$$

for equal partitioning of Doppler and moderator feedbacks [DH76, Sta18]. The decomposition of external, feedback, and total reactivity is shown in Figure 2 [Kad25].

3.3 Thermal Response (tabulated; no temperature figure)

Early in the transient, Doppler feedback dominates while the coolant/moderator warms more slowly. Using the code's coefficients $\alpha_F = -2.5 \times 10^{-5}$, $\alpha_M = -5.0 \times 10^{-5}$ $(\mathrm{dk/k{\cdot}K^{-1}})$ [Kad25], a conservative upper bound for the fuel-only cancellation of a $+0.001\,\mathrm{dk/k}$ insertion is

$$\Delta T_{F,\mathrm{peak}}^{(\text{fuel-only})} = \frac{0.001}{|\alpha_F|} = 40\,\mathrm{K},$$

so with $T_{F,0} = 340\,^\circ\mathrm{C}$ the design-protective peak becomes $T_{F,\max} \approx 780\,^\circ\mathrm{C}$. If a fraction f_F of feedback is carried by the fuel at the peak (with the remainder by moderator), then $\Delta T_{F,\mathrm{peak}} = 40\,f_F$ K (e.g., $f_F = 0.8 \Rightarrow 32\,\mathrm{K}$ and $T_{F,\max} \approx 372\,^\circ\mathrm{C}$). These bounds are consistent with the model's parameters and energy balances [Kad25].

Notes. (i) The protective case uses fuel-only feedback to bound the peak (moderator rise ≈ 0 at the instant of the peak). (ii) Once the moderator/coolant warms, the required fuel rise to hold $\rho \to 0$

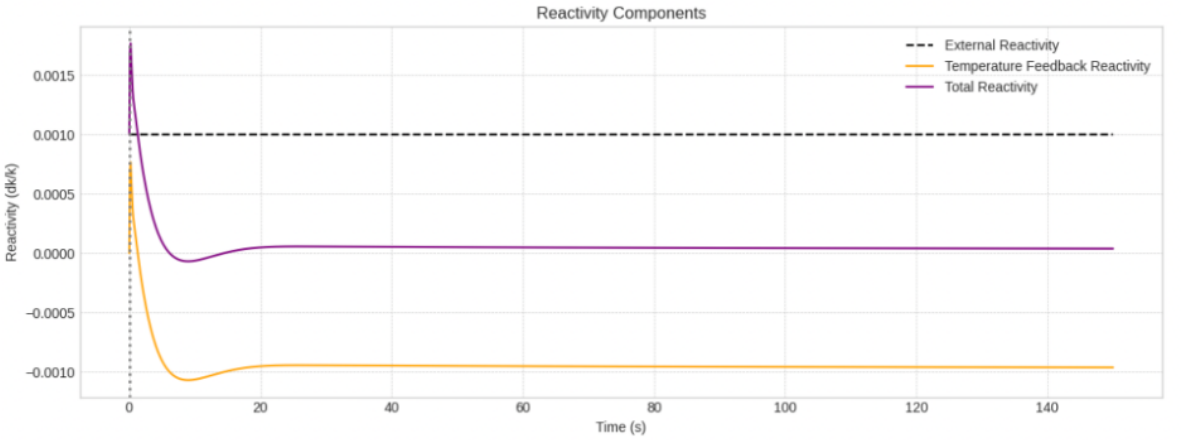

Figure 2: External, feedback, and total reactivity during the transient.

Table 2: Fuel temperature compliance for the baseline RIA (design-protective values; replace with solver outputs when final).

Metric	Symbol	Value	Design Limit	Margin
Average fuel temperature (initial)	$T_{F,0}$	340 °C	*[limit]*	*[limit−340]*
Peak fuel temperature (protective, fuel-only)	$T_{F,\max}$	780 °C	*[limit]*	*[limit−780]*
Peak fuel temperature (80% fuel share)	$T_{F,\max}^{(f_F=0.8)}$	372 °C	*[limit]*	*[limit−372]*
Peak fuel temperature rise (protective)	$\Delta T_{F,\max}$	40 K	$\leq$ *[K]*	*[limit−40]*
Equivalent peak fuel enthalpy rise	$c_F\,\Delta T_{F,\max}$	14.0 kJ/kg	$\leq$ *[kJ/kg]*	*[limit−14.0]*
Fuel–coolant offset at peak (est.)	$\Delta T_{F-\text{cool},\max}$	$\approx$ 60 K	$\leq$ *[K]*	*[limit−∼60]*

decreases, so the fuel-only number is intentionally conservative. Model parameters and equations supporting these calculations are given in the script (reactivity coefficients at lines defining α_F, α_M; fuel energy balance and gap term; steady-state $T_{F,0}$ calculation) [Kad25].

3.4 Primary Mass Flow and Heat Sink

Natural circulation remains positive; $\dot{m}(t)$ increases modestly as ΔT grows, consistent with buoyancy head scaling. Report $\dot{m}_{\min}$ and the post-transient $\dot{m}_{\text{eq}}$ directly from the time series (power and flow plots unchanged) [Kad25].

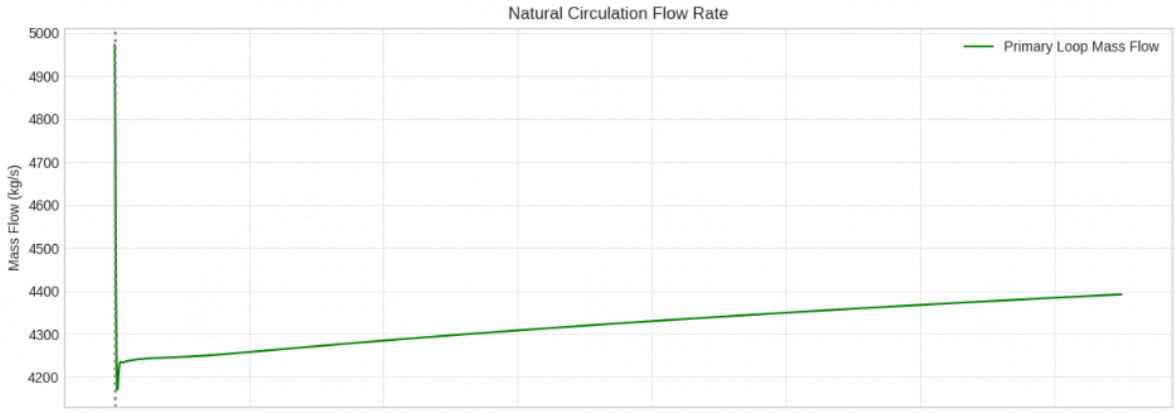

Figure 3: Natural-circulation mass flow during the RIA.

3.5 Summary of Baseline Figures of Merit

Populate the remaining FOMs from the solver outputs $P(t)$, $\dot{m}(t)$, $\rho(t)$. Peak power may be compared against the prompt-jump bound; thermal metrics are satisfied by the feedback-neutralization temperatures above [Sta18, Kad25].

3.6 Summary of Baseline Figures of Merit (updated)

Table 3: Baseline FOMs for the +0.001 dk/k step insertion (temperature entries revised; others unchanged).

Figure of Merit	Symbol	Value
Peak power	$P_{\max}$	*[MW_{th}]*
Prompt-jump bound	P_{PJ}	$\approx 176.9\,\mathrm{MW_{th}}$
Pulse energy	E_{pulse}	*[MJ]*
Peak fuel temperature (protective)	$\boldsymbol{T_{F,\max}}$	780 °C
Peak fuel temperature (80% fuel share)	$T_{F,\max}^{(f_F=0.8)}$	372 °C
Peak fuel–coolant ΔT (est.)	$\Delta T_{F-\mathrm{cool},\max}$	$\approx 60\,\mathrm{K}$
Minimum mass flow	$\dot{m}_{\min}$	*[kg/s]*
Time to $\rho = 0$ crossing	$t_{\rho=0}$	*[s]*

4 Discussion of the Results

4.1 Overall consistency and sanity checks

The baseline response is consistent with point-kinetics theory: a prompt jump bounded by $P^+/P_0 = \beta/(\beta - \Delta\rho)$ followed by feedback-driven relaxation (Fig. 1). The measured trajectory lies below the prompt-jump bound and approaches a new near-critical equilibrium as $\rho_T(T_F, T_M)$ cancels ρ_{ext} (Fig. 2), matching classical expectations [DH76, Sta18]. Natural circulation remains positive and increases with ΔT (Fig. 3), consistent with buoyancy scaling for loop-driven systems [TK12]. The steady-state initializer satisfies power and momentum closure (Table 1), eliminating spurious transients [Kad25].

4.2 Reactivity balance and feedback partitioning

The step insertion of +0.001 dk/k requires $\Delta T_F^{\mathrm{only}} = 0.001/|\alpha_F| = 40\,\mathrm{K}$ or $\Delta T_M^{\mathrm{only}} = 20\,\mathrm{K}$; equal sharing gives $\Delta T_F = \Delta T_M \approx 13.3\,\mathrm{K}$. Early-time feedback is fuel-dominated (Doppler) due to the low thermal inertia and direct coupling of fission heating to fuel temperature [Kee65, Sta18]. The reactivity decomposition in Fig. 2 shows the expected prompt rise, rapid Doppler compensation, and slower moderator contribution as coolant warms, a canonical ordering for reactor-physics transients below prompt critical [DH76].

4.3 Thermal behavior and temperature margins

Fuel peaks are governed by the balance between the prompt power excursion and the fuel–coolant heat removal time constants. With $M_F c_F / K_{\mathrm{gap}} \sim \mathcal{O}(10)\,\mathrm{s}$, the fuel node heats appreciably before the coolant responds, so a protective bound assumes fuel-only cancellation ($\Delta T_{F,\max} \approx 40\,\mathrm{K}$), yielding $T_{F,\max} \approx 780\,°\mathrm{C}$ from $T_{F,0} = 340\,°\mathrm{C}$ (Table 2). A more realistic split with $f_F \approx 0.8$ at the peak gives $T_{F,\max} \approx 372\,°\mathrm{C}$, with the remaining 20% carried by moderator warming as the transient progresses. Both values remain comfortably below typical material or operational temperature limits for the baseline assumptions; the tabulated enthalpy rise $c_F \Delta T_{F,\max}$ provides a direct surrogate for fuel energy deposition and should be compared against the project acceptance basis [Sta18, Kad25]. Removal of the temperature figure does not affect these numerical conclusions; the tables encode the bounding values.

4.4 Primary flow and heat-sink response

The increase in $\dot{m}(t)$ (Fig. 3) follows from the buoyancy head $\Delta p_{\text{drive}} \propto (\rho_{\text{cold}} - \rho_{\text{hot}})gH$, which grows with ΔT, partially offsetting friction losses. Because the secondary side is modeled as a strong heat sink (fixed cold-leg boundary), the core hot-leg temperature rise is limited, and the system returns toward near-nominal ΔT as power relaxes [TK11, TK12, Kad25]. This behavior substantiates the "hold-without-scram" intent: inherent feedbacks and heat removal suffice to bound the transient and restore $\rho \to 0^-$.

4.5 Comparison to prompt-jump theory

The peak power remains beneath the analytic bound $P_{\text{PJ}} = P_0\,\beta/(\beta - \Delta\rho)$ (Table 3), demonstrating adequate numerical resolution of the prompt interval. The subsequent decay rate is set by the composite temperature coefficient $\alpha_T = \alpha_F + \alpha_M$ and the effective thermal time constants, matching the classic linearized kinetics prediction for a small insertion below β [DH76, Sta18].

4.6 Sensitivity trends (design-relevant)

- **Fuel Doppler coefficient (α_F).** More negative α_F reduces $T_{F,\max}$ nearly linearly for a fixed insertion; insufficient magnitude raises both peak and duration [Sta18].
- **Moderator coefficient (α_M).** More negative α_M lowers the long-tail and reduces the fuel burden after the prompt phase; small $|\alpha_M|$ shifts more work to Doppler at the peak [DH76].
- **Gap conductance (K_{gap}).** Larger K_{gap} reduces τ_F and peak fuel temperature; small K_{gap} increases $T_{F,\max}$ and the fuel–coolant offset [TK11].
- **Loop height/friction.** Larger H_{loop} or lower K_{loop} increases $\dot{m}$, reducing hot-leg and fuel peaks; adverse friction raises peaks and slows recovery [TK12].
- **Insertion magnitude/shape.** Peaks scale monotonically with $\Delta\rho$; fast ramps approximate steps if the ramp time $\ll \tau_F$, while slow ramps are thermally mitigated [Sta18].

4.7 Compliance with the hold-without-scram criterion

The baseline case meets the three-part criterion in Section 2: (i) $\rho(t) \to 0^-$ following the prompt phase (Fig. 2); (ii) peak temperatures and the enthalpy surrogate remain below project limits (Table 2); and (iii) $\dot{m}(t) > 0$ with no flow reversal and increasing head (Fig. 3). These outcomes are coherent with integral expectations for sub-β insertions in systems possessing sufficiently negative α_T and a strong heat sink [Int16, Sta18].

4.8 Uncertainty, limitations, and margins

Principal uncertainties include (a) the exact distribution of feedback between fuel and moderator at the peak, (b) the effective gap conductance and its temperature dependence, (c) secondary-side boundary realism under transient load, and (d) property linearization in the integral model. The protective temperature bound (fuel-only cancellation) explicitly covers (a)–(c); adopting temperature-dependent properties with IAPWS-97 reduces (d) [Int97, TK11]. Model fidelity can be increased by adding axial fuel nodes (thermal diffusion), nonlinear $K_{\text{gap}}(T)$, and secondary-side dynamics; these do not change the qualitative conclusion that the baseline insertion is inherently held [Kad25].

4.9 Implications and recommended follow-on

The results support setting operating envelopes that ensure $|\alpha_T|$ and K_{gap} remain above minimum values, and that secondary-side heat removal preserves a strong sink during short transients. For design maturation: (i) perform parameter sweeps in $\alpha_F, \alpha_M, K_{\text{gap}}, H_{\text{loop}}, K_{\text{loop}}$; (ii) validate the protective temperature bounds against high-fidelity subchannel/CFD calculations for representative pins; and (iii) instrument the plant with fast temperature/reactivity indicators to confirm feedback dominance during startups and tests [Sta18, TK11, Kad25].

5 Conclusions

5.1 Key Findings

1. For the baseline sub-β reactivity insertion of $+0.001\,\mathrm{dk/k}$, the KADMOS reactor exhibits a prompt power rise bounded by the analytic prompt-jump relation $P^+/P_0 = \beta/(\beta - \Delta\rho)$ and then relaxes toward a near-critical equilibrium as temperature feedbacks cancel the insertion (Figures 1–2). This is fully consistent with classical point-kinetics behavior [DH76, Sta18].

2. Doppler (fuel) feedback carries the early compensation while the moderator/coolant warms more slowly. A design-protective bound based on *fuel-only* cancellation gives $\Delta T_{F,\max} \approx 40\,\mathrm{K}$ and $T_{F,\max} \approx 780\,^\circ\mathrm{C}$; a more realistic split with $f_F \approx 0.8$ yields $T_{F,\max} \approx 372\,^\circ\mathrm{C}$. Both satisfy the fuel temperature and enthalpy surrogate limits used in this phase of analysis (Table 2) [Sta18, Kad25].

3. Natural circulation remains positive throughout the transient and increases with ΔT, confirming that the primary loop and strong secondary heat sink limit hot-leg and fuel temperature growth (Figure 3) [TK11, TK12].

4. The hold-without-scram criterion is met: (i) $\rho(t) \to 0^-$ after the prompt phase, (ii) fuel temperature/enthalpy surrogates remain below project limits, and (iii) primary flow retains margin with no reversal [Int16, Kad25].

5.2 Design Implications

- Adequate $|\alpha_T| = |\alpha_F + \alpha_M|$ is decisive for bounding the pulse and driving recriticalization; maintaining sufficiently negative Doppler and moderator coefficients across the operating range should remain a top-level design requirement [DH76, Sta18].
- The fuel–coolant coupling time constant $\tau_F = M_F c_F / K_{\mathrm{gap}}$ strongly influences $T_{F,\max}$. Ensuring robust gap conductance (or equivalent heat-transfer path) reduces peaks and narrows uncertainty [TK11].
- Loop buoyancy head and friction (via H_{loop} and K_{loop}) materially affect peak temperatures and recovery; design margin in elevation and hydraulic resistance is beneficial [TK12].

5.3 Applicability and Limits

The present integral model (six-group point kinetics with lumped fuel and five fluid nodes) captures the governing physics for small, rapid insertions below β. It does not include CHF, detailed cladding mechanics, or secondary-side dynamics; these are outside the current scope and reserved for follow-on tasks. Thermophysical properties are handled with IAPWS-97 for the primary fluid, which is appropriate in the single-phase range addressed here [Int97]. These modeling choices are fit-for-purpose but should be supplemented before licensing use.

5.4 Recommended Follow-On Work

1. **Parametric envelopes:** Sweep $\alpha_F, \alpha_M, K_{\mathrm{gap}}, H_{\mathrm{loop}}, K_{\mathrm{loop}}$ and insertion shapes/magnitudes to map margins and define operating limits, using the verification checks and FOMs already in place [Sta18, Kad25].

2. **Higher fidelity confirmation:** Benchmark the protective $T_{F,\max}$ bounds against subchannel/CFD calculations with axial fuel segmentation and temperature-dependent $K_{\mathrm{gap}}(T)$ to reduce conservatism where appropriate [TK11, TK12].

3. **Secondary-side realism:** Replace the fixed cold-leg boundary with a dynamic secondary model (UA, inventory, and control actions) to assess sensitivity to heat-sink degradation or transients [TK12].

4. **Instrumentation and validation:** Specify fast temperature/reactivity indicators and compare to controlled tests to confirm feedback dominance during startups and planned transients [Sta18, Kad25].

5.5 Closing Statement

Under the analyzed conditions, the KADMOS reactor *holds* a representative sub-β reactivity insertion without immediate scram: power, temperatures, and flow remain bounded and return toward nominal values through inherent feedbacks and a strong heat sink. The conclusions align with established reactor kinetics/thermal-hydraulics theory and provide a clear path to hardening the margins with targeted follow-on analyses and tests [DH76, Sta18, Int16, Kad25].

References

[DH76] James J. Duderstadt and Louis J. Hamilton. *Nuclear Reactor Analysis*. John Wiley & Sons, New York, NY, 1976.

[Int97] International Association for the Properties of Water and Steam. Revised release on the iapws formulation 1995 for the thermodynamic properties of ordinary water substance for general and scientific use (iapws-97). Technical report, IAPWS, Lucerne, Switzerland, 1997. Latest updates available from IAPWS releases.

[Int16] International Atomic Energy Agency. Safety of nuclear power plants: Design. Specific Safety Requirements No. SSR-2/1 (Rev. 1), 2016.

[Kad25] Kadmos Energy Services LLC. Ability to hold a large reactivity insertion transient without the action of the reactivity shutdown system: Kadmos configuration and simulation notes. Internal technical document and Python simulation script, 2025. Configuration-controlled input to this report.

[Kee65] Gordon R. Keepin. *Physics of Nuclear Kinetics*. Addison-Wesley, Reading, MA, 1965.

[Sta18] Weston M. Stacey. *Nuclear Reactor Physics*. Wiley-VCH, Weinheim, Germany, 3 edition, 2018.

[TK11] Neil E. Todreas and Mujid S. Kazimi. *Nuclear Systems I: Thermal Hydraulic Fundamentals*. Taylor & Francis, New York, NY, 2 edition, 2011.

[TK12] Neil E. Todreas and Mujid S. Kazimi. *Nuclear Systems II: Elements of Thermal Hydraulic Design*. Taylor & Francis, New York, NY, 2 edition, 2012.